

PagP Activation in the Outer Membrane Triggers R3 Core Oligosaccharide Truncation in the Cytoplasm of *Escherichia coli* O157:H7*

Abigail E. Smith^{1,#}, Sang-Hyun Kim^{2,5,#}, Feng Liu¹, Wenyi Jia^{2,6}, Evgeny Vinogradov³,
Carlton L. Gyles⁴, and Russell E. Bishop^{1,2}

¹Department of Biochemistry and Biomedical Sciences, McMaster University, Hamilton, ON, L8N 3Z5 Canada; ²Departments of Laboratory Medicine & Pathobiology, and Biochemistry, University of Toronto, Toronto, ON, M5S 1A8 Canada; ³Institute for Biological Sciences, National Research Council, Ottawa, ON, K1A OR6 Canada; ⁴Department of Pathobiology, Ontario Veterinary College, University of Guelph, Guelph, ON, N1G 2W1 Canada.

Running Head: PagP activation controls R3 core truncation

Address correspondence to: Russell E. Bishop, Department of Biochemistry & Biomedical Sciences, McMaster University, Hamilton, ON, Canada L8N 3Z5. Telephone: 905 525 9140 Ext. 28810. FAX: 905 522 9033. E-mail: bishopr@mcmaster.ca

[#]These authors made equal contributions to this work.

⁵Present address: The National Primate Research Center, KRIBB, Daejeon 305-806, South Korea.

⁶Present address: Shanghai Asia United Antibody Medical Co. LTD., Zhang Jiang Hi-tech Park, Pudong, Shanghai 201203, China.

The *Escherichia coli* outer membrane phospholipid:lipid A palmitoyltransferase PagP is normally a latent enzyme, but it can be directly activated in outer membranes by lipid redistribution associated with a breach in the permeability barrier. We now demonstrate that a lipid A myristate deficiency in an *E. coli* O157:H7 *msbB* mutant constitutively activates PagP in outer membranes. The lipid A myristate deficiency is associated with hydrophobic antibiotic sensitivity and, unexpectedly, with serum sensitivity, which resulted from O-antigen polysaccharide absence due to a cytoplasmically determined truncation at the R3 core oligosaccharide's first outer core glucose unit. Mutational inactivation of *pagP* in the myristate-deficient lipid A background aggravated the hydrophobic antibiotic sensitivity as a result of losing a partially compensatory increase in lipid A palmitoylation, while simultaneously restoring serum resistance and O-antigen attachment to intact lipopolysaccharide. Complementation with either wild-type *pagP* or catalytically inactive

pagPSer77Ala alleles restored the R3 core truncation. However, the intact lipopolysaccharide was preserved after complementation with an internal deletion *pagPΔ5-14* allele, which mostly eliminates a periplasmic amphipathic α -helical domain, but fully supports cell surface lipid A palmitoylation. Our findings indicate that activation of PagP not only triggers lipid A palmitoylation in the outer membrane, but also separately truncates the R3 core oligosaccharide in the cytoplasm. We discuss the implication that PagP might function as an apical sensory transducer, which can be activated by a breach in the outer membrane permeability barrier.

Like most enteric Gram-negative bacteria, *Escherichia coli* surrounds its cytoplasmic membrane with a reticulated peptidoglycan exoskeleton (murein) and an outer membrane (OM), which demarcates the so-called periplasmic space. The enterobacterial OM is an asymmetric lipid bilayer in which lipopolysaccharide (LPS) exclusively lines the external leaflet while phospholipids line the inner leaflet (1,2).

The asymmetric lipid organization provides a permeability barrier to hydrophobic antibiotics and detergents encountered in the natural and host environments. Although hydrophobic antibiotics can freely permeate through phospholipid bilayers, negative charges in LPS are bridged by Mg^{2+} -ions to create tight lateral packing interactions, which largely prevent permeation (3,4). According to current models, perturbations of OM lipid asymmetry can result from the migration of phospholipids into the external leaflet to create localized rafts of phospholipid bilayers, which render bacteria susceptible to hydrophobic antibiotics (5,6).

The LPS is a tripartite molecule consisting of the hydrophobic anchor lipid A (endotoxin), the core oligosaccharide, which is divided into the inner and outer core regions, and the O-antigen polysaccharide (7). The so-called rough LPS includes only the lipid A-core and is usually distinguished from the smooth LPS that also includes O-antigen. The O-antigen can provide bacterial resistance to serum by preventing deposition of the complement cascade's membrane attack complex (8).

The entire LPS structure is assembled within three distinct subcellular compartments; namely, the cytoplasmic membrane, the periplasmic space, and the OM (9). The Raetz pathway for lipid A biosynthesis includes nine Lpx enzymes, which convert uridine diphosphate *N*-acetylglucosamine (UDP-GlcNAc) into a β -1',6-linked disaccharide of glucosamine (GlcN) (7). The lipid A molecule is phosphorylated at positions 1 and 4', and acylated with *R*-3-hydroxymyristate in ester linkage at positions 3 and 3', and in amide linkage at positions 2 and 2' (Fig. 1). Attachment at position 6' of two 3-deoxy-D-manno-oct-2-ulosonic acid (Kdo) sugars, which belong to the innermost region of the inner core, is followed by secondary acylation reactions to create the so-called acyloxyacyl linkages. Attachment of laurate at position 2' is usually followed by

attachment of myristate at position 3', which is catalyzed by the myristoyltransferase MsbB (LpxM) (10). Each of these enzymatic reactions take advantage of cytoplasmic energy-rich biosynthetic precursors (7).

The *waa* (*rfa*) operons encode cytoplasmic enzymes needed for the step-wise assembly of any one of the five known core oligosaccharides (K-12, and R1-R4) that can exist in *E. coli*. Although ~170 distinct O-antigens have been identified in *E. coli* alone, they are all assembled on the lipid carrier analog of dolichol phosphate known as bactoprenol phosphate. Translocation of the lipid A-core and bactoprenol diphosphate-O-antigen to the periplasmic surface of the inner membrane can be followed by polymerization of the O-antigen polysaccharide with its subsequent *en bloc* ligation to the outer core. At this periplasmic stage, several regulated partial modifications can occur on both lipid A and the inner core, and include the addition of phosphoethanolamine (PEtN), derived from phosphatidylethanolamine, and 4-amino-4-deoxy-L-arabinose (L-Ara4N), derived from bactoprenol phosphate-L-Ara4N (11). These modifications provide resistance to polymyxin B and can be induced by mildly acidic growth conditions, antimicrobial peptides, or Mg^{2+} -limitation, which together activate the PhoP/PhoQ and PmrA/PmrB two-component signal transduction pathways (12,13).

E. coli K-12 strains generally synthesize rough LPS lacking O-antigen polysaccharide unless certain genetic factors are exogenously provided (14). In contrast, smooth LPS with attached O157 polysaccharide is synthesized in enterohemorrhagic *E. coli* O157:H7. This most common serotype of Shiga toxin-producing *E. coli* is associated with hemorrhagic colitis and hemolytic-uremic syndrome in humans (15). The core oligosaccharide of *E. coli* O157:H7 is of the R3 type, which is distinctly different from

K-12 in the outer core regions (16). The lipid A and inner core structures of the R3 and K-12 LPS are largely identical, with the exception of a few important differences that can be attributed to enzymes encoded in the plasmid pO157 *shf* locus.

The conserved inner core includes, in addition to the two Kdo units, three units of L-glycero-D-manno-heptose (Hep), which can be modified with phosphate and/or PETN moieties at key positions (Fig. 1). A defining feature of the R3 inner core is the partial modification of HepIII by an α -1,7-linked GlcNAc unit, which is controlled by the *shf* locus-encoded glycosyltransferase WabB (16). Additionally, under normal laboratory growth conditions, where the corresponding enzymes of *E. coli* K-12 are found to be latent (17), *E. coli* O157:H7 introduces significant amounts of PETN into the lipid A phosphate groups (18). Finally, *E. coli* O157:H7 possesses two homologues of the *msbB* gene: *msbB1* encoded on the chromosome, which is equivalent to the single *msbB* gene of *E. coli* K-12, and *msbB2* encoded on the *shf* locus. Both *msbB* orthologues must be inactivated to create a myristate deficiency in the lipid A of *E. coli* O157:H7, and this is associated with reduced virulence (19) as similarly occurs in *msbB* deficient *Shigella flexneri* (20). The only ascribed function for the single *msbB2* gene is in the persistence of *E. coli* O157:H7 in its agricultural and bovine reservoirs (21).

The entire LPS structure is transported across the periplasmic space and delivered to the OM external leaflet where lipid A can be further modified (11). PagP is the only known OM enzyme of LPS biosynthesis in *E. coli* and it is controlled by PhoP/PhoQ (22). PagP acylates the lipid A position-2 R-3-hydroxymyristate chain with a phospholipid-derived palmitoyl group (23,24), which provides resistance to cationic antimicrobial peptides (25-27) and attenuates the ability of LPS to trigger host defences through the TLR4 pathway (28,29). PagP structure and dynamics demonstrate

that the palmitate recognition pocket, known as the hydrocarbon ruler, is only accessible from the OM external leaflet and, thus, requires aberrant translocation of phospholipids into the external leaflet (30-32). Indeed, PagP remains dormant in the OM until perturbations to lipid asymmetry, which compromise the OM permeability barrier, directly trigger PagP activity (33). PagP has been proposed to function as a sentinel that can be activated by a breach in the OM permeability barrier (34). We now demonstrate that a lipid A myristoylation mutant of enterohemorrhagic *E. coli* O157:H7, but not a similar mutant from *E. coli* K-12, necessarily triggers PagP activity in the OM to exert control on cytoplasmic enzymes that determine its characteristic R3 core oligosaccharide structure. PagP sensory transduction is not controlled by its cell surface catalytic machinery, but depends instead on its periplasmic amphipathic α -helix.

Experimental Procedures

Materials- $^{32}\text{P}_i$ was purchased from PerkinElmer Life Sciences. Antibiotics and galactose (Gal) were obtained from Sigma. Pyridine, methanol, and 88% formic acid were obtained from Mallinckrodt. Chloroform was purchased from EM Science. Glass-backed Silica Gel 60 thin layer chromatography (TLC) plates were from Merck. The QIAprep spin miniprep, Qiaquick polymerase chain reaction (PCR) purification, and QIAEX II gel extraction kits were obtained from Qiagen. High-fidelity PCR was performed with a proof-reading DNA polymerase (Advantage-HF2 PCR kit, BD Biosciences-Clontech, CA). Restriction endonucleases, T4 DNA ligase, and dNTP were obtained from Fermentas. Bacto MacConkey agar was obtained from Difco Laboratories. All other materials were obtained from commercial sources.

Bacterial Strains, Plasmids, and Growth Conditions- The bacterial strains and

plasmids used in this study are described in Table 1. Cells were generally grown at 37 °C in Luria Bertani (LB) broth. Antibiotics were added when necessary at final concentrations of 12 µg/ml for tetracycline, 20 µg/ml for chloramphenicol and gentamycin (Gm), 100 µg/ml for ampicillin (Ap) and streptomycin (Str), and 40 µg/ml for kanamycin. Antibiotic concentrations were reduced by a factor of 10 during selection of the hypersensitive *E. coli* O157:H7 strain 4303-TM. Single colonies were inoculated from plates into 5 ml of liquid medium and grown at 37 °C overnight to stationary phase. A 1% inoculum was then subcultured into the same medium and allowed to resume growth at 37 °C. Cultures were adjusted with EDTA using a stock solution of 250 mM EDTA, pH 8.0, which had been sterilized by using a 0.2-µm filter.

DNA Manipulations- Restriction enzyme digestions, ligations, transformations, and DNA electrophoresis were performed as described (35). The oligonucleotide primers used for DNA sequencing and PCR gene amplification were manufactured by Invitrogen. Purification of plasmids, PCR products, and restriction fragments was performed with the QIAprep, QIAquick, and QIAEX II kits, respectively, according to the manufacturer's instructions (Qiagen). Genomic DNA was purified using the Easy-DNA kit (Invitrogen). DNA sequencing was performed at the ACGT Corp. sequencing facility (Toronto, Ontario, Canada).

Mutant constructions- An allelic exchange method was employed for creation of a *pagP::aacCI* mutation in the double *msbB* mutant (4304-DM) of *E. coli* O157:H7 strain 4304 (Table 1). In brief, the *pagP* gene was amplified from wild type strain 4304 by PCR with primers CrcA (Forward: ATGAGCTCAGGTTGACGATA) and CrcR (Reverse: TTGAATTCTTGCTGACGTATC) to yield a 1.3 kb product. The amplicon was cloned into the pGEM-T vector and the

recombinant plasmid (pCrcAT) was digested with *KpnI*, which cuts a single site near the middle of the *pagP* gene. For insertion of the non-polar Gm-cassette, the *KpnI* fragment containing the *aacCI* gene was purified from pUCGM carrying the *aacCI* gene in the multiple cloning site. The plasmid resulting from ligation of the *aacCI* gene into pCrcAT was used as template DNA for a high-fidelity PCR with proof-reading DNA polymerase and the primer pair CrcA and CrcR. The 2.1 kb amplicon was purified for blunt-end ligation with the pRE107 vector digested with *SmaI*. The resulting suicide vector construct was named pR7Crc-Gm. The SM10 donor *E. coli* was transformed with the pR7Crc-Gm plasmid harboring the mutated (*pagP::aacCI*) allele. Strain SM10 (pR7Crc-Gm) was mated with 4304-DM and incubated at 37 °C overnight on blood agar plates. This mating procedure was subsequently repeated using the wild-type strain 4304 to generate a single *pagP::aacCI* mutant. The exconjugants were selected on LB agar plates containing appropriate antibiotics (Str^R + Gm^R). The resulting exconjugants were spread on LB agar plates containing 7% sucrose and Gm and incubated at 30 °C in order to select isolates that had undergone a double crossover. A few selected colonies were purified and the potential *pagP::aacCI* mutants (Gm^r and Ap^s) were tested by PCR for confirmation of the mutated allele. The primer pair of CrcA and CrcR was used for amplification of the *pagP::aacCI* allele from the mutants. The expected size (2.1 kb) of the amplicon in the mutants was compared with that of the wild type *pagP* gene (1.3 kb) by 1% agarose-gel electrophoresis. The resulting *pagP::aacCI* mutant of *E. coli* 4304-DM was named 4304-TM, while that of *E. coli* 4304 was named 4304-PM (Table 1). The *msbB::Tn5* allele in the *E. coli* K-12 donor strain BMS67C12 was transferred by P1 transduction to the *E. coli* K-12 strain WJ0124 to create strain SK1061 (Table 1).

A temperature-sensitive P1 *cmr*-100 lysate of BMS67C12 (36) was prepared as described elsewhere (18) and then mixed with *E. coli* WJ0124. The resulting *msbB::Tn5* mutant of WJ0124 was verified by PCR.

Analysis of lipid A by TLC- Analysis of lipid A compositional profiles was done by TLC separation of ^{32}P -labelled lipid A species released from a mild acid hydrolysis procedure, applied to bacteria cultured with or without EDTA treatment (33,37).

LPS preparation and SDS-PAGE analysis- LPS was prepared on a small scale from SDS-proteinase K treated whole-cell lysates (38). Large-scale LPS preparations were made by the phenol-chloroform-petroleum ether extraction procedure as described elsewhere (39). The LPS was then separated on a 16% Tricine SDS-PAGE gel (Novex, San Diego, Calif.) and was visualized by silver staining (40). PAGE conditions were adjusted as recommended by the manufacturer.

NMR spectroscopy- NMR spectra were recorded at 25 °C in D_2O on a Varian UNITY INOVA 500 instrument, using acetone as reference for proton (2.225 ppm) and carbon (31.5 ppm) spectra. Varian standard programs for COSY, NOESY (mixing time of 400 ms), TOCSY (spinlock time 120 ms), HSQC, and gHMBC (long-range transfer delay 100 ms) were used.

Isolation of the core oligosaccharide- LPS (30 mg) was hydrolyzed with 2% acetic acid (3h, 100 °C). Lipid was removed by centrifugation and soluble products separated by gel chromatography on Sephadex G-50 to yield core oligosaccharide (15 mg) and a low molecular mass fraction. The core was additionally purified by anion-exchange chromatography on a Hitrap Q column (Amersham) using a gradient of NaCl from 0 to 1M over 1 h, and the major acidic core fraction was desalted by gel chromatography.

Hydrazine O-deacylation of the LPS- LPS (20 mg) was dissolved in anhydrous

hydrazine (1 ml) and kept at 60 °C for 1h, cooled and poured into acetone (50 ml). Precipitate was collected, washed with acetone, dissolved in water and freeze-dried to give O-deacylated LPS (12 mg).

Monosaccharide analysis- Hydrolysis was performed with 4M trifluoroacetic acid (110 °C, 3h), and monosaccharides were conventionally converted into alditol acetates and analyzed by gas chromatography on an Agilent 6850 chromatograph equipped with a DB-17 (30 mm x 0.25 mm) fused-silica column using a temperature gradient from 180 °C (2 min) to 240 °C at 2 °C/min.

Mass spectrometry- ESI/MS spectra were obtained using a Micromass Quattro spectrometer in 50% acetonitrile with 0.2% formic acid at a flow rate of 15 $\mu\text{l}/\text{min}$ with direct injection. The 5 kV electrospray ionization voltage was used.

Immunoblotting- The LPS samples of 4304, DM (*msbB1/msbB2*), and DM (pBAD-B2) were resolved by 16% Tricine SDS-PAGE and transferred to a nitrocellulose membrane. The membrane was blocked with 5% skim milk in standard Tris-buffered saline-Tween 20 buffer. Anti-O157 rabbit serum (Difco) and anti-rabbit IgG coupled with horseradish peroxidase (Sigma) were used as primary and secondary antibodies, respectively. For chemiluminescent detection, the ECL detection kit was used according to the manufacturer's instructions (Amersham).

Construction of plasmids for phenotypic complementation- The *waaG* gene of *E. coli* O157:H7 was amplified by PCR using 4304-WT genomic DNA and the two primers called WG24-Kpn (forward: GACAGGTACGTCGTTATGGTACCTGCTTTTG) and WG24-H3 (reverse: CTTTACCGCGCCAAGCTTGGCAAACGGCTC), and then cloned into an arabinose-inducible pBAD24 expression vector digested with *KpnI* and *HindIII*. The insertion was verified by agarose gel electrophoresis and the construct was named pWG24. Also, the

galU gene of *E. coli* O157:H7 was amplified by PCR using 4304-WT genomic DNA and the two primers called GalU-H3 (forward: TGCATTACAAGCTTATGTCGGCTGG) and GalU-Sal (reverse: GTCGATTGGTCGACGCCGTTTCGTG). The 1.1 kb amplicon including the endogenous promoter region was digested with *HindIII* and *SalI*, inserted into pACYC184 digested with the same restriction enzymes, and the resulting plasmid was named pGU184. The *pagP* gene of *E. coli* O157:H7 was amplified by a high fidelity PCR using genomic DNA and the two primers called Pag24-Kpn (forward: TGGTCACAAATGGTACCGAGTAAATATGTCCG) and Pag24-H3 (reverse: GAAGTTACTAAAGCTTCATTTGTCTCAA). The approximately 600 bp amplicon was digested with *KpnI* and *HindIII*, and cloned into an arabinose-inducible pBAD24 expression vector digested with *KpnI* and *HindIII*. The insertion was verified by agarose gel electrophoresis and the construct was named pEP24. LPS samples were prepared from the bacterial transformants carrying pEP24 cultured on LB plates containing 0.2% arabinose for the induction of expression of the cloned *pagP*_{O157} gene. Plasmid pACPagPSer77Ala was prepared by site directed mutagenesis as described previously (31), except using pACPagP as template. Plasmid pAA101 containing the *galETK* genes was obtained and used for complementation of 4304-DM (41). Exogenous Gal (final conc. 0.5%) was added into LB agar plates, and used for culturing derivatives of 4304-DM.

Serum resistance assay- A serum resistance assay was conducted by a method described elsewhere (42) with minor modifications. In brief, aliquots of 90 μ l of nonimmune calf serum were prepared and kept on ice before use. A 10 μ l suspension of bacteria in PBS (pH 7.4) containing approximately 1×10^5 CFU/ml was added to the 90 μ l of normal serum and to heat-inactivated serum (56 °C

for 30 min). A 10 μ l volume of zero-hour sample was immediately taken for 10-fold serial dilution in PBS, and each dilution was plated onto trypticase-soy agar (TSA). The remaining mixture was incubated at 37 °C for 1 hour. After 1-hour incubation, a series of 10-fold dilutions in PBS was made from both sets of mixtures (normal and heat-inactivated serum). Each dilution was plated onto TSA and incubated overnight at 37 °C. Viable counts were calculated as mean values of at least two independent experiments with the same non-immune calf serum. Viability (%) was normalized in proportion to the value (100%) obtained from the zero-hour counts of each strain. **Antibiotic sensitivity assays-** For the determination of MICs for vancomycin and novobiocin, the microdilution method was exploited as recommended by the National Committee for Clinical Laboratory Standards (43). In brief, two-fold serial dilutions of the antibiotic were made in Mueller-Hinton (MH) broth (pH 7.2) in 96-well microtitre plates. Then, bacteria at a final concentration of 5×10^5 CFU/ml in a volume equal to that of the antibiotic-containing MH broth were added to each well. The MICs were recorded as the lowest concentration of the antibiotic that did not allow visible bacterial growth after 20 h incubation at 37 °C.

Membrane extraction of PagP- Extraction of PagP from membranes was performed using lauroyldimethylamine-*N*-oxide (LDAO) as described previously (23), and specific activity determined by a standard TLC assay (24).

RESULTS

MsbB deficiency triggers *PagP* activity in the OM of *E. coli* O157:H7. We have employed a TLC-based mild acid hydrolysis procedure (33,37) to analyze ³²P-labeled lipid A from both *E. coli* K-12 and O157:H7 wild-type strains together with

their myristate and/or palmitate deficient lipid A mutants (Fig. 2). The procedure disrupts the labile ketosidic bond and liberates the first Kdo sugar from lipid A without affecting the distribution of acyl-chains. One artefact of the procedure is the partial dephosphorylation of the anomeric lipid A carbon at position 1. Roughly two thirds of lipid A in *E. coli* K-12 contains a monophosphate group while the remaining third contains a diphosphate group at this position. The small amount of 1-dephosphorylated lipid A migrates the furthest among the three species on the TLC plate (Fig. 2). *E. coli* O157:H7 shows a similar profile, except that an additional species containing PEtN at position 1 is also apparent (18). Each of these species represents a hexa-acylated lipid A that exhibits a typical 4+2 acyl-chain distribution, with two acyloxylacyl groups on the distal GlcN unit and two unmodified primary *R*-3-hydroxymyristate chains on the proximal GlcN unit.

Despite the presence of PagP in the OM, the enzyme remains dormant when OM lipid asymmetry is maintained (33). EDTA can promote the migration of phospholipids into the OM external leaflet, which sensitizes cells to hydrophobic antibiotics, by chelating Mg^{2+} -ions that normally neutralize negative charges and promote tight LPS-LPS packing interactions (4-6). PagP activity triggered by EDTA occurs nearly instantaneously, is dependent on lipid trafficking, and is independent of *de-novo* protein synthesis (33). Less than 5% of the lipid A 1-phosphate contains palmitate under normal growth conditions, but approximately 20% palmitoylation is achieved after a brief EDTA treatment. The additional hepta-acylated lipid A species that are apparent after EDTA treatment are clearly absent in the *pagP* mutant derivatives of the wild-type strains (Fig. 2).

MsbB deficiency generates a penta-acylated lipid A characterized by the absence of myristate in *E. coli* K-12 (37).

EDTA treatment of the K-12 *msbB* mutant promotes palmitoylation to a similar extent as in the wild-type strain, but it generates a new hexa-acylated lipid A species characterized by an atypical 3+3 acyl chain distribution. In this case, a single acyloxylacyl group and a single unmodified primary *R*-3-hydroxymyristate chain are found on each GlcN unit. The two types of hexa-acylated lipid A migrate at similar positions, but the 4+2 acyl chain distribution migrates perceptibly faster on the TLC plate (Fig. 2). The positions of the palmitoylated lipid A species in the *msbB*-deficient strains are made apparent by their absence in the mutant derivatives that also lack *pagP*. In addition to the PEtN-modified species, two new slowly migrating penta-acylated species are apparent in the *msbB*- and *pagP*-deficient *E. coli* O157:H7 mutant, which are not present in the corresponding *E. coli* K-12 mutant. The species migrating just above the 1-diphosphate coincides with the 4' L-Ara4N derivative, and the most polar substituent likely coincides with two species doubly modified by L-Ara4N at position 4' and either diphosphate or PEtN at position 1 (37,44). Lipid A myristoylation is a requirement for L-Ara4N addition in *E. coli* K-12 (45), but this does not appear to be true in *E. coli* O157:H7. Interestingly, lipid A palmitoylation occurred constitutively in the *msbB*-deficient *E. coli* O157:H7 mutant (Fig. 2). This observation suggests that *msbB*-deficiency in *E. coli* O157:H7 serves to increase lipid A palmitoylation in the absence of EDTA by introducing its own perturbation of lipid asymmetry, which directly triggers the activity of pre-existing PagP in the OM.

MsbB deficiency is associated with an OM permeability defect in *E. coli* O157:H7. Structural considerations of PagP in relation to OM bilayer organization predict that phospholipids must migrate into the external leaflet during PagP catalysis (22). We find that the *msbB* deficiency in *E. coli* O157:H7, which is associated with

PagP activation, is also associated with increased sensitivity to vancomycin and the hydrophobic antibiotic novobiocin. Mutation of *pagP* in this *msbB*-deficient background aggravates the antibiotic sensitivity (Table 2), which suggests that lipid A palmitoylation can partially compensate for the absence of myristate in lipid A. Previous studies of *msbB* mutants have revealed increased sensitivity to antibiotics in *Salmonella*, but not in *E. coli* K-12 (46,47), and our observations confirm these latter findings (Table 2). We also observed slow growth and poor growth of *msbB*- and *msbB/pagP*-deficient *E. coli* O157:H7, respectively, on lactose MacConkey agar plates, which contain bile salts that select against organisms with a compromised OM permeability barrier (not shown). The association of PagP activation with hydrophobic antibiotic and bile salt sensitivity is consistent with earlier predictions that OM permeability to hydrophobic compounds can result from the migration of phospholipids into the OM external leaflet (5,6).

MsbB deficiency truncates the R3 core oligosaccharide of *E. coli* O157:H7. In order to evaluate the status of LPS glycosylation in the wild-type and *msbB*-deficient *E. coli* O157:H7 bacteria, we extracted LPS from cells and visualized it by silver staining after Tricine SDS-PAGE (Fig. 3). The results identify a complete lipid A core that includes the attached O-antigen repeats characteristic of smooth *E. coli* O157:H7 LPS. Unexpectedly, the *msbB*-deficient mutant completely lacks O-antigen repeats and appears to possess a truncated lipid A-core, which can be restored by complementation with an *msbB2* expression plasmid. A minor species migrating above the truncated lipid A-core might suggest the presence of a single O-antigen unit, but this was ruled out after immunoblotting with O157 antiserum (Fig. 3C). We verified that the LPS core in our *E. coli* K-12 *msbB*

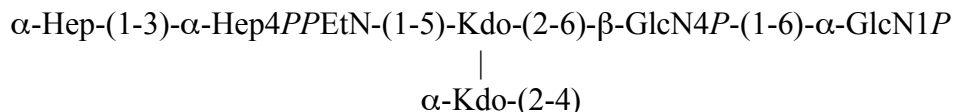
mutant is intact by observing that it can be modified with a *Klebsiella pneumoniae* O-antigen polysaccharide (48), which can be attached to the outer core when the required genes are expressed in *E. coli* K-12 (data not shown).

To further characterize the nature of the R3 core truncation, we purified it for biochemical analysis. Monosaccharide analysis of the whole LPS, by gas chromatography of alditol acetates, showed the presence of Hep and GlcN in an approximate 1:1 ratio. The core oligosaccharide appeared to contain only Hep and was further analyzed by NMR spectroscopy. A set of 2D NMR spectra (COSY, TOCSY, NOESY, HSQC, HMBC) was recorded and all major proton and carbon signals were assigned. Spectra contained signals of two Hep residues and a Kdo, as well as of PPEtN. Kdo was present in several forms with dominating α -pyranoside; Hep residue E also showed several sets of signals due to the attachment to Kdo variants. The sequence of the monosaccharides was determined using NOE and HMBC data, which contained correlations (H-H and H-C) F1-E3 and E1-C5. The ^{31}P spectrum of the core contained two signals at -9 and -9.5 ppm, correlating with E4 and EtN-1 protons. This agrees with the attachment of EtNPP to O-4 of Hep E, which also led to the low-field shift of H-4 and C-4 of Hep E to 4.58 and 72.6 ppm, respectively (compared with non-phosphorylated H-4 and C-4 of Hep F at 3.88 and 67.1 ppm) (Fig. 4). The ESI mass spectrum of the core contained peaks at m/z 824.3 (main species, full molecule with PEtN; calculated 824.5 Da), 806.3 (its anhydro Kdo derivative; calculated 806.5 Da), 701.3 (same molecule without PEtN; calculated 701.5 Da), and 683.3 (its anhydro Kdo derivative; calculated 683.4 Da). Thus, the core has the following structure:



In order to confirm the structure of the LPS, ESI MS of *O*-deacylated LPS was recorded. It contained doubly and triply charged peaks of the expected full structure (Hep)₂(Kdo)₂(GlcN)₂(P)₄(EtN)₁(C14OH)₂ (1980.5 Da), the structure without PEtN

(1857.5 Da) and without PPEtN (1777.5 Da). All peaks were accompanied by Na-adducts (+22). Thus, the chemical data show that the LPS had the following carbohydrate backbone:



These observations are consistent with a core truncated at the level of the first outer core glucose (Glc) and with only a partial PPEtN modification at HepI (Fig. 1).

Both the R3 and K-12 core structures include three Hep units attached to KdoI (14). Partial modification of KdoII with PEtN is also observed when *E. coli* is cultured under calcium-enriched conditions (49,50). The R3 and K-12 core structures share in common the first outer core Glc, which is attached by an α -1,3-linkage with HepII (Fig. 1). This first Glc unit is required for complete phosphorylation of HepI (51), which can be followed by partial modification with PEtN. HepI phosphorylation is a prerequisite for attachment of HepIII, which is itself a prerequisite for phosphorylation of HepII (52). Although HepII phosphorylation is nearly stoichiometric in *E. coli* K-12, its presence is only partial and mutually exclusive with the attachment of GlcNAc by WabB at HepIII in *E. coli* O157:H7 (Fig. 1) (16). Consequently, biosynthetic deficiencies in the first Glc will not only manifest the absence of the outer core and *O*-polysaccharide, but will also necessarily exclude the inner core GlcNAc, HepIII, and Hep phosphate groups. These findings demonstrate that our observed core truncation most likely represents a deficiency in the cytoplasmic incorporation

of the first outer core Glc, rather than the action of a series of previously unreported extracellular hydrolytic enzymes.

Mutation of pagP restores R3 core structure in msbB-deficient E. coli O157:H7. We found that *pagP* mutations suppress the truncated core phenotype and restore smooth LPS to the *msbB*-deficient *E. coli* O157:H7 mutant (Fig. 5). A low copy recombinant pACPagP plasmid (33) introduced into the myristate and palmitate deficient lipid A mutant restores the truncated LPS observed in the absence of the *pagP* mutation. If the *pagP* mutation can restore smooth LPS to the *msbB*-deficient *E. coli* O157:H7, we reasoned that *O*-antigen-mediated resistance to serum should also be restored to wild-type levels as a consequence. We were able to demonstrate that only the *msbB*-deficient mutant, and not the wild-type *E. coli* O157:H7 or its mutant deficient in both *msbB* and *pagP*, displayed sensitivity to killing by serum that is characteristic of *O*-antigen-deficient *E. coli* K-12 (Table 3). These findings clearly dissociate hydrophobic antibiotic sensitivity (a consequence of lipid A underacylation) from serum sensitivity (a consequence of R3 core truncation).

Signal transduction is mediated by the PagP amphipathic α -helix. Since overproduction of PagP could not produce an R3 core truncation in the wild-type strain

(data not shown), we realized that R3 core truncation in *E. coli* O157:H7 is a consequence of an epistatic interaction between *msbB* and *pagP*. We were concerned that the production of an atypical lipid A structure with the 3+3 acyl chain distribution, which contains palmitate and lacks myristate, might somehow interfere with OM biogenesis and inadvertently trigger the periplasmic stress response. In *E. coli* K-12 subjected to a temperature shift from 30°C to 42°C, PagP-catalyzed lipid A palmitoylation has been implicated in the activation of the extracytoplasmic function or ECF sigma factor σ^E (53). However, we could show that a catalytically inactive *pagPSer77Ala* allele restores the R3 core truncation just as effectively as the wild-type *pagP* (Fig. 5), but only the latter is capable of palmitoylating lipid A *in vivo* (Fig. 6). Therefore, the observed R3 core truncation is not simply an artefact of producing an atypical lipid A molecular subtype.

PagP is an 8-stranded antiparallel β -barrel that is preceded by an amino terminal amphipathic α -helix (30,31). The active site is located at the cell surface, but the amphipathic α -helix lies along the periplasmic surface of the OM (Fig. 5C). We have previously created internal deletions that remove sections of the amphipathic α -helix, but still allow the signal peptide to direct the export and assembly of PagP in the OM. We reported that OM lipid A palmitoylation, catalyzed by the amphipathic α -helix deletion constructs, could be detected at levels that were indistinguishable from a similar wild-type PagP construct (33). We now demonstrate that a *pagP Δ 5-14* allele, which removes most of the amphipathic α -helix, is fully active in the palmitoylation of lipid A under normal conditions (Fig. 6), but it is no longer capable of restoring the R3 core truncation (Fig. 5). Interestingly, the R3 core truncation correlates only with the presence of the PagP amphipathic α -helix

and not with differences in the pattern of lipid A acylation (Figure 5B). Since we have already established that OM permeability depends on the lipid A acylation pattern (Table 2), the R3 core truncation is not likely a secondary consequence of PagP's influence on the barrier function of the OM. These findings suggest that PagP activation in the OM, initiated by the *E. coli* O157:H7 *msbB* deficiency, not only triggers lipid A palmitoylation at the cell surface, but also separately triggers R3 core oligosaccharide truncation in the cytoplasm through the action of the PagP amphipathic α -helix.

The PagP amphipathic α -helix is a post-assembly membrane clamp in vivo. Huysmans and colleagues have recently reported studies of PagP folding in liposomes (54), which verify our earlier conclusions that the PagP amphipathic α -helix is not essential for membrane assembly (33). Interestingly, the liposome folding studies also indicate that the PagP amphipathic α -helix functions as a post-assembly clamp to stabilize PagP in membranes after folding is complete (54). To determine whether the *pagP Δ 5-14* allele encodes a protein that is more easily extracted from membranes *in vivo*, we took advantage of our previous findings that wild-type PagP can be solubilized from membranes by serial extractions with increasing amounts of the detergent LDAO (23). As predicted by the liposome studies, PagP Δ 5-14 is much more sensitive to detergent extraction than is wild-type PagP (Fig. 7). The critical micellar concentration (cmc) for LDAO is ~0.025%, and at the lowest concentration of LDAO tested (twice the cmc) we observed nearly complete extraction of PagP Δ 5-14 from membranes, whereas the wild-type PagP was only completely extracted at 20 times the cmc (Fig. 7). Although the bulk of the wild-type PagP specific activity was found in the soluble fraction, as previously reported (23),

PagP Δ 5-14 was not appreciably active in the soluble fraction, which suggests that the PagP amphipathic α -helix can have an important role in stabilizing PagP against detergent inactivation.

Furthermore, we have previously observed that increasing PagP expression by transformation with the pACPagP plasmid can increase the level of lipid A 1-phosphate palmitoylation to roughly 20%, but subsequent EDTA treatment results in hyperpalmitoylation up to 90% (33). Indeed, hyperpalmitoylation was borne out here during EDTA treatment of the pACPagP transformant shown in Fig. 6, but this was not the case for the pACPagP Δ 5-14 transformant, which appears to be insensitive to EDTA-activation in the *msbB*-deficient background. Importantly, under conditions where the R3 core truncation is induced (without detergent extraction of membranes and without EDTA treatment of cells), PagP Δ 5-14 palmitoylates lipid A to a degree that cannot be distinguished from wild-type PagP (Fig. 6 and 7). Since lipid A palmitoylation dictates that the PagP Δ 5-14 enzyme is properly assembled in the OM, cytoplasmic R3 core truncation is likely controlled by the PagP periplasmic amphipathic α -helix through a cell envelope sensory transduction mechanism.

UDP-Glc depletion is linked to R3 core truncation in msbB-deficient E. coli O157:H7. We reasoned that the core truncation observed in *msbB*-deficient *E. coli* O157:H7 could be caused by a deficiency in the expression of the WaaG glucosyltransferase responsible for addition of the first outer core Glc residue (51). However, expression of WaaG from a recombinant plasmid did not correct the core truncation (data not shown). We then investigated the possibility that the WaaG donor substrate UDP-Glc might be limiting. Indeed, we found that expression from a recombinant GalU plasmid of UDP-Glc pyrophosphorylase, which replenishes the cytoplasmic pool of UDP-Glc (55,56), could

largely restore smooth LPS to the *msbB*-deficient *E. coli* O157:H7 mutant (Fig. 8). Similarly, exogenous Gal, which can be converted to UDP-Glc by the Leloir pathway (57), could also restore smooth LPS (Fig. 8). The Leloir pathway enzymes cloned on a recombinant GalETK plasmid did not appear to be limiting (data not shown), but this probably reflects the reversible nature of these reactions, which simultaneously produce and consume UDP-Glc. These observations support the hypothesis that the *msbB*-deficient *E. coli* O157:H7 mutant is limiting in UDP-Glc, which likely blocks WaaG and all reactions that depend on WaaG, ultimately leading to the observed R3 core truncation.

DISCUSSION

Taken together, our observations demonstrate that PagP activation depends on *msbB*-deficiency, and that R3 core truncation depends on activated PagP. Signal transduction might connect PagP in the OM with cytoplasmic R3 core metabolism. In principle, regulation of the cytoplasmic pool of UDP-Glc could be exerted at the level of gene expression, through covalent enzyme modification, or through allosteric control of enzyme activity (56,58). The notion that an OM protein can control gene transcription is not entirely unprecedented. The OM ferric citrate receptor FecA is known to control transcription of key components of the iron uptake machinery in response to ligand binding events that occur in the OM (59). At this stage, we can only speculate on how PagP influences the cytoplasmic pool of UDP-Glc or on the nature of the intrinsic differences between *E. coli* K-12 and O157:H7 cell envelopes that led us to our conclusions by necessarily studying the enterohemorrhagic bacterium.

Natural conditions that trigger PagP in wild-type cells, including *E. coli* K-12 and other species that encode PagP

homologues, might include Mg^{2+} -limitation, exposure to cationic amphipathic peptides, or any other condition known to perturb OM lipid asymmetry. The narrow distribution of PagP among mostly pathogenic organisms could indicate that the biological trigger is somehow associated with host-pathogen interactions (22). Conceivably, an R3 core truncation might be of a selective advantage if it facilitates exchange of host and pathogen factors, and is appropriately triggered by prior contact made between host epithelial and *E. coli* O157:H7 cell surfaces. In bacillary dysentery, shortening the length of *Shigella* cell surface LPS by modifying the O-antigen structure is believed to facilitate the association of a key type-III secretion system with human epithelial cells (60).

Given that the R3 core truncation has not been observed previously in *E. coli* O157:H7 pathogenesis, we must concede that its biological significance remains unresolved. The possibility remains that constitutive activation of PagP in the *msbB*-deficient background excessively diverts the pool of UDP-Glc toward other cell surface components, such as L-Ara4N and colanic acid (58) or trehalose and membrane-derived oligosaccharides (56), and thereby truncates the R3 core as an unintended consequence. Regardless of its biological significance, we wish to emphasize here that the R3 core truncation provides a useful phenotypic probe, which has revealed the apical component of what appears to be a

previously unrecognized signal transduction pathway in *pagP*-encoding Gram-negative bacteria.

In the present study, we suspect that lipid A lacking myristate is initially glycosylated normally and transported to the OM where it perturbs lipid asymmetry specifically in *E. coli* O157:H7. By activating PagP in the OM, the *msbB* deficiency initiates signal transduction to exert negative control on key cytoplasmic enzymes of R3 core biosynthesis, which only then leads to R3 core truncation (Fig. 9). The constitutive state of PagP activation serves to deplete the cell of all LPS bearing the attached O-antigen. Only this model has the power of predicting that a *pagP* mutation would restore smooth LPS and serum resistance to the *msbB*-deficient *E. coli* O157:H7, while simultaneously aggravating a defect in OM lipid asymmetry associated with lipid A underacylation and hydrophobic antibiotic sensitivity. We conclude that OM activation of PagP not only triggers lipid A palmitoylation, to partially compensate for lipid A underacylation in the *E. coli* O157:H7 *msbB* mutant, but also separately triggers signal transduction across three distinct cellular compartments through the action of the periplasmic amphipathic α -helix. Discovering the downstream signaling components that respond to the activated state of PagP will provide fertile ground for future research.

REFERENCES

1. Kamio, Y., and Nikaido, H. (1976) *Biochemistry* **15**(12), 2561-2570
2. Nikaido, H. (2003) *Microbiol Mol Biol Rev* **67**(4), 593-656
3. Schindler, M., and Osborn, M. J. (1979) *Biochemistry* **18**(20), 4425-4430
4. Leive, L. (1974) *Ann N Y Acad Sci* **235**(0), 109-129
5. Nikaido, H., and Nakae, T. (1979) *Adv Microb Physiol* **20**, 163-250
6. Nikaido, H., and Vaara, M. (1985) *Microbiol Rev* **49**(1), 1-32
7. Raetz, C. R., and Whitfield, C. (2002) *Annu Rev Biochem* **71**, 635-700
8. Joiner, K. A. (1985) *Curr Top Microbiol Immunol* **121**, 99-133
9. Bishop, R. E. (2005) *Contrib Microbiol* **12**, 1-27

10. Clementz, T., Zhou, Z., and Raetz, C. R. (1997) *J Biol Chem* **272**(16), 10353-10360
11. Raetz, C. R., Reynolds, C. M., Trent, M. S., and Bishop, R. E. (2007) *Annu Rev Biochem* **76**, 295-329
12. Groisman, E. A. (2001) *J Bacteriol* **183**(6), 1835-1842
13. Bader, M. W., Sanowar, S., Daley, M. E., Schneider, A. R., Cho, U., Xu, W., Klevit, R. E., Le Moual, H., and Miller, S. I. (2005) *Cell* **122**(3), 461-472
14. Heinrichs, D. E., Yethon, J. A., and Whitfield, C. (1998) *Mol Microbiol* **30**(2), 221-232
15. Tarr, P. I., Gordon, C. A., and Chandler, W. L. (2005) *Lancet* **365**(9464), 1073-1086
16. Kaniuk, N. A., Vinogradov, E., Li, J., Monteiro, M. A., and Whitfield, C. (2004) *J Biol Chem* **279**(30), 31237-31250
17. Gibbons, H. S., Kalb, S. R., Cotter, R. J., and Raetz, C. R. (2005) *Mol Microbiol* **55**(2), 425-440
18. Kim, S. H., Jia, W., Parreira, V. R., Bishop, R. E., and Gyles, C. L. (2006) *Microbiology* **152**(Pt 3), 657-666
19. Kim, S. H., Jia, W., Bishop, R. E., and Gyles, C. (2004) *Infect Immun* **72**(2), 1174-1180
20. D'Hauteville, H., Khan, S., Maskell, D. J., Kussak, A., Weintraub, A., Mathison, J., Ulevitch, R. J., Wuscher, N., Parsot, C., and Sansonetti, P. J. (2002) *J Immunol* **168**(10), 5240-5251
21. Yoon, J. W., Lim, J. Y., Park, Y. H., and Hovde, C. J. (2005) *Infect Immun* **73**(4), 2367-2378
22. Bishop, R. E. (2005) *Mol Microbiol* **57**(4), 900-912
23. Bishop, R. E., Gibbons, H. S., Guina, T., Trent, M. S., Miller, S. I., and Raetz, C. R. (2000) *Embo J* **19**(19), 5071-5080
24. Khan, M. A., Neale, C., Michaux, C., Pomes, R., Prive, G. G., Woody, R. W., and Bishop, R. E. (2007) *Biochemistry* **46**(15), 4565-4579
25. Guo, L., Lim, K. B., Poduje, C. M., Daniel, M., Gunn, J. S., Hackett, M., and Miller, S. I. (1998) *Cell* **95**(2), 189-198
26. Robey, M., O'Connell, W., and Cianciotto, N. P. (2001) *Infect Immun* **69**(7), 4276-4286
27. Pilione, M. R., Pishko, E. J., Preston, A., Maskell, D. J., and Harvill, E. T. (2004) *Infect Immun* **72**(5), 2837-2842
28. Kawasaki, K., Ernst, R. K., and Miller, S. I. (2004) *J Biol Chem* **279**(19), 20044-20048
29. Miller, S. I., Ernst, R. K., and Bader, M. W. (2005) *Nat Rev Microbiol* **3**(1), 36-46
30. Ahn, V. E., Lo, E. I., Engel, C. K., Chen, L., Hwang, P. M., Kay, L. E., Bishop, R. E., and Prive, G. G. (2004) *Embo J* **23**(15), 2931-2941
31. Hwang, P. M., Choy, W. Y., Lo, E. I., Chen, L., Forman-Kay, J. D., Raetz, C. R., Prive, G. G., Bishop, R. E., and Kay, L. E. (2002) *Proc Natl Acad Sci U S A* **99**(21), 13560-13565
32. Hwang, P. M., Bishop, R. E., and Kay, L. E. (2004) *Proc Natl Acad Sci U S A* **101**(26), 9618-9623
33. Jia, W., Zoeiby, A. E., Petruzzello, T. N., Jayabalasingham, B., Seyedirashti, S., and Bishop, R. E. (2004) *J Biol Chem* **279**(43), 44966-44975
34. Bishop, R. E. (2007) *Biochim Biophys Acta* (in press)
35. Sambrook, J., Fritsch, E. F., and Maniatis, T. (1989) *Molecular cloning : a laboratory manual*, 2nd Ed., Cold Spring Harbor Laboratory, Cold Spring Harbor, N.Y.
36. Somerville, J. E., Jr., Cassiano, L., and Darveau, R. P. (1999) *Infect Immun* **67**(12), 6583-6590
37. Zhou, Z., Lin, S., Cotter, R. J., and Raetz, C. R. (1999) *J Biol Chem* **274**(26), 18503-18514

38. Hitchcock, P. J., and Brown, T. M. (1983) *J Bacteriol* **154**(1), 269-277
39. Galanos, C., Luderitz, O., and Westphal, O. (1969) *Eur J Biochem* **9**(2), 245-249
40. Tsai, C. M., and Frasch, C. E. (1982) *Anal Biochem* **119**(1), 115-119
41. Edwards-Jones, B., Langford, P. R., Kroll, J. S., and Yu, J. (2004) *Microbiology* **150**(Pt 4), 1079-1084
42. Helmuth, R., Stephan, R., Bunge, C., Hoog, B., Steinbeck, A., and Bulling, E. (1985) *Infect Immun* **48**(1), 175-182
43. NCCLS. (2002) **Vol.22**(No.6), M31-A32. Wayne, Pa.
44. Zhou, Z., Ribeiro, A. A., and Raetz, C. R. (2000) *J Biol Chem* **275**(18), 13542-13551
45. Tran, A. X., Lester, M. E., Stead, C. M., Raetz, C. R., Maskell, D. J., McGrath, S. C., Cotter, R. J., and Trent, M. S. (2005) *J Biol Chem* **280**(31), 28186-28194
46. Vaara, M., and Nurminen, M. (1999) *Antimicrob Agents Chemother* **43**(6), 1459-1462
47. Murray, S. R., Bermudes, D., de Felipe, K. S., and Low, K. B. (2001) *J Bacteriol* **183**(19), 5554-5561
48. Clarke, B. R., and Whitfield, C. (1992) *J Bacteriol* **174**(14), 4614-4621
49. Kanipes, M. I., Lin, S., Cotter, R. J., and Raetz, C. R. (2001) *J Biol Chem* **276**(2), 1156-1163
50. Reynolds, C. M., Kalb, S. R., Cotter, R. J., and Raetz, C. R. (2005) *J Biol Chem* **280**(22), 21202-21211
51. Yethon, J. A., Vinogradov, E., Perry, M. B., and Whitfield, C. (2000) *J Bacteriol* **182**(19), 5620-5623
52. Yethon, J. A., Heinrichs, D. E., Monteiro, M. A., Perry, M. B., and Whitfield, C. (1998) *J Biol Chem* **273**(41), 26310-26316
53. Tam, C., and Missiakas, D. (2005) *Mol Microbiol* **55**(5), 1403-1412
54. Huysmans, G. H., Radford, S. E., Brockwell, D. J., and Baldwin, S. A. (2007) *J Mol Biol* **373**(3), 529-540
55. Marolda, C. L., and Valvano, M. A. (1996) *Mol Microbiol* **22**(5), 827-840
56. Bohringer, J., Fischer, D., Mosler, G., and Hengge-Aronis, R. (1995) *J Bacteriol* **177**(2), 413-422
57. Holden, H. M., Rayment, I., and Thoden, J. B. (2003) *J Biol Chem* **278**(45), 43885-43888
58. Grangeasse, C., Obadia, B., Mijakovic, I., Deutscher, J., Cozzone, A. J., and Doublet, P. (2003) *J Biol Chem* **278**(41), 39323-39329
59. Harle, C., Kim, I., Angerer, A., and Braun, V. (1995) *Embo J* **14**(7), 1430-1438
60. West, N. P., Sansonetti, P., Mounier, J., Exley, R. M., Parsot, C., Guadagnini, S., Prevost, M. C., Prochnicka-Chalufour, A., Delepierre, M., Tanguy, M., and Tang, C. M. (2005) *Science* **307**(5713), 1313-1317
61. Edwards, R. A., Keller, L. H., and Schifferli, D. M. (1998) *Gene* **207**(2), 149-157
62. Schweizer, H. D. (1993) *Biotechniques* **15**(5), 831-834

FOOTNOTES

*The authors wish to thank Janet Liao of the University of Guelph, for excellent technical support. We gratefully acknowledge Miguel Valvano and Cristina Marolda, for advice on LPS analysis, and Chris Whitfield, Janet Wood, Jun Yu, and Richard Darveau for providing bacterial strains, plasmids, and phage. S. H. K. was supported by the Canadian Institutes of Health Research (CIHR) training programme (Post-Doctoral) on the structure and function of membrane

proteins linked to disease (University of Toronto). CIHR Operating Grant MOP-84329 funded work in the laboratory of R. E. B.

The abbreviations used are : L-Ara4N, 4-amino-4-deoxy-L-arabinose; Ap, ampicillin; cmc, critical micellar concentration; Gal, galactose; Glc, glucose; GlcNAc, *N*-acetylglucosamine; GlcN, glucosamine; Gm, gentamycin; Hep, *L-glycero-D-manno*-heptose; Kdo, 3-deoxy-D-*manno*-oct-2-ulosonic acid; LB, Luria-Bertani; LDAO, lauroyldimethylamine-*N*-oxide; LPS, lipopolysaccharide; MIC, minimal inhibitory concentration; MH, Mueller-Hinton; OM, outer membrane; PBS, phosphate buffered saline; PCR, polymerase chain reaction; PEtN, phosphoethanolamine; PL, phospholipids; Str, streptomycin; TSA, trypticase-soy agar; TLC, thin-layer chromatography; UDP, uridine diphosphate.

FIGURE LEGENDS

Fig. 1. *Structure of lipid A and the inner R3 core oligosaccharide of E. coli O157:H7.* Lipid A is an acylated and phosphorylated disaccharide of GlcN linked by a β -1',6-glycosidic bond. Three of the four primary *R*-3-hydroxymyristate chains can be modified with secondary acyloxyacyl groups. MsbB can incorporate a myristate chain and a palmitate chain can be partially incorporated by PagP (red). Partial modification of the lipid A phosphate groups with diphosphate, PEtN, and L-Ara4N can also be observed. The inner core consists of two Kdo and three Hep sugars, which can be substituted with phosphate and PEtN groups. GlcNAc is a unique feature of the R3 inner core of *E. coli* O157:H7, but the remaining inner core structures and lipid A are virtually identical in *E. coli* K-12, which has a distinctly different outer core structure and no O-antigen. Structures shown in blue were found in this study to be absent in the *msbB*-deficient mutant of *E. coli* O157:H7. Dashed bonds specify partial substitutions.

Fig. 2. *TLC analysis of ^{32}P lipid A profiles after mild-acid hydrolysis.* Lipid A was labeled with $^{32}P_i$ and isolated from cells by mild acid hydrolysis. Wild-type *E. coli* O157:H7 (4304) and K-12 (MC1061) were analyzed in comparison with their *msbB* and/or *pagP* mutant derivatives. Cultures were grown for 150 min and adjusted with or without 25 mM EDTA for an additional 5 min. The isolated lipid A species were separated by TLC and visualized with a PhosphorImager. The main species of lipid A that were identified previously by mass spectrometry are indicated to the left of the figure and include the 4'-monophosphate (1-OH), the 1,4'-bis-phosphate (1-OP), the 1-diphosphate (1-O-PP), the 1-diphosphoryl-EtN (1-O-PPEtN), and the 4'-L-Ara4N lipid A species. The penta-, hexa-, and hepta-acylated derivatives of each lipid A species are also indicated to the left of the figure (panel A). Schematic representations (panel B) reveal the relative migration of certain lipid A molecular subtypes in the TLC plate. The fastest migrating species (hepta-acyl 1-OH) has the most number of acyl chains and the least number of polar groups. The acylation patterns for the 1-OH lipid A species are shown as an example, which reveals that the penta-acylated derivative migrates most slowly. Of the two faster migrating hexa-acylated species with 4+2 and 3+3 acyl-chain distributions, the 4+2 species migrates perceptibly faster and this difference becomes accentuated as more polar groups are added. The effect of adding various polar substituents is shown schematically only for the penta-acylated lipid A species, but relative migrations for all combinations of acyl-chain distributions and polar substituents can be deduced by extrapolation from these selected examples. Relative migrations are not drawn exactly to scale and palmitate is shown in red.

Fig. 3. *Tricine SDS-PAGE analysis of E. coli O157:H7 LPS.* LPS was isolated from wild-type *E. coli* O157:H7, its *msbB*-deficient mutant, and the same mutant complemented with an *MsbB2* expression plasmid. The LPS was resolved by Tricine SDS PAGE and visualized by silver staining. Different resolution of the O-antigen ladder pattern was observed in 12% gels (panel A) and 16% gels (panel B). The position of O-antigen units was identified by immunoblotting with O157-specific antisera (panel C).

Fig. 4. *NMR chemical shift assignments of truncated E. coli O157:H7 LPS.* Assignment of the HSQC correlation spectrum for the core oligosaccharide. Cross-peaks marked in green refer to CH groups while those marked in red refer to CH₂ groups (panel A). ¹H and ¹³C NMR chemical shift values (δ, ppm) for the core oligosaccharide (panel B).

Fig. 5. *Complementation of the truncated R3 core oligosaccharide of msbB-deficient E. coli O157:H7.* Silver stained 16% Tricine SDS-PAGE analysis of LPS isolated from wild-type *E. coli* O157:H7 strain 4303 and its lipid A acylation mutants deficient in either *msbB* or both *msbB* and *pagP*. Bacteria transformed with pACPagP, pACPagPSer77Ala, and pACPagPΔ5-14 are indicated (panel A). The presence (+) or absence (-) of the PagP periplasmic amphipathic α-helix, and of lipid A acylated by palmitate or myristate, as deduced from figures 2 and 6, is indicated (panel B). Structural model of PagP derived from the crystal structure (PDB: 1THQ). The first seven N-terminal residues are disordered in the crystal structure, but the approximate position of the Δ5-14 deletion in the periplasmic amphipathic α-helix (red), and the cell surface catalytic residues, are indicated. The bound LDAO detergent molecule (yellow) identifies the hydrocarbon ruler. The aromatic belts define the boundaries of the OM, where LPS occupies the external leaflet and phospholipids (PL) occupy the periplasmic leaflet (panel C).

Fig. 6. *TLC analysis of ³²P lipid A profiles after mild-acid hydrolysis.* Lipid A was labeled with ³²P_i and isolated from cells by mild acid hydrolysis as described in figure 2. In this figure, hexa refers to the 3+3 acyl chain distribution.

Fig. 7. *LDAO extraction of PagP specific activity from membranes.* *E. coli* WJ0124 transformed with pACPagP or pACPagPΔ5-14 was serially extracted from membranes using increasing amounts of LDAO and the specific activity remaining in the membranes was determined.

Fig. 8. *Complementation of the truncated R3 core oligosaccharide of msbB-deficient E. coli O157:H7.* Silver stained 16% Tricine SDS-PAGE analysis of LPS isolated from wild-type *E. coli* O157:H7 and its lipid A acylation mutant deficient in *msbB*. Bacteria were cultured in the presence and absence of exogenous Gal, and with or without complementation by a plasmid encoding GalU.

Fig. 9. *Model for PagP-mediated control of R3 core oligosaccharide structure.* PagP is the only known OM enzyme of LPS biosynthesis in *E. coli* and it serves to transfer a palmitate chain from a phospholipid to lipid A with the production of a lysophospholipid by-product. Lipid A palmitoylation attenuates endotoxin signalling through the host TLR4 pathway and affords resistance to cationic antimicrobial peptides. PagP measures the phospholipid palmitate chain in its hydrocarbon ruler, which is only accessible from the OM external leaflet. A defect in cytoplasmic lipid A myristoylation triggers PagP activity in the OM of *E. coli* O157:H7. Activated PagP not only palmitoylates lipid A at the cell surface, to partially compensate for

lipid A underacylation, but also separately initiates signal transduction through its periplasmic amphipathic α -helix. Signal transduction exerts negative control on the cytoplasmic UDP-Glc pool and leads to a truncation of the R3 core oligosaccharide.



Table 1. Bacterial strains and plasmids used in this study.

Strains/plasmids	Description ^a	Source
<i>E. coli</i> O157:H7		
4304	Wild-type (phage-type 14), (Str ^r)	(19)
4304-DM	4304 Δ <i>msbB1</i> , Δ <i>msbB2</i> (Str ^r) [<i>msbB1/2</i>]	(19)
4304-PM	4304 <i>pagP::aacC1</i> (Str ^r , Gm ^r) [<i>pagP</i>]	this study
4304-TM	4304 Δ <i>msbB1</i> , Δ <i>msbB2</i> , <i>pagP::aacC1</i> (Str ^r , Gm ^r) [<i>msbB1/2/pagP</i>]	this study
<i>E. coli</i> K-12		
MC1061	F ⁻ , λ ⁻ , <i>araD139</i> , Δ (<i>ara-leu</i>)7697, Δ (<i>lac</i>)X74, <i>galU</i> , <i>galK</i> , <i>hsdR2</i> (r _k -m _k +), <i>mcrB1</i> , <i>rpsL</i>	(33)
WJ0124	MC1061 <i>pagP::amp</i> [<i>pagP</i>]	(33)
SK1061	MC1061 <i>msbB::Tn5</i> , <i>pagP::amp</i> [<i>msbB/pagP</i>]	this study
MC- <i>msbB</i>	MC1061 <i>msbB::Tn5</i> [<i>msbB</i>]	(18)
BMS67C12	<i>msbB::Tn5</i> mutant of JM83 (Km ^r)	(36)
SM10	<i>thr</i> , <i>leu</i> , <i>tonA</i> , <i>lacY</i> , <i>supE</i> , <i>recA::RP4-2-Tc::Mu</i> , Km ^r , λ <i>pir</i>	(61)
plasmids		
pGEM-T	PCR product cloning vector	Promega
pUCGM	Gm ^r cassette (<i>aacC1</i>)-containing plasmid	(62)
pR7Crc-Gm	pRE107 carrying <i>pagP::aacC1</i>	this study
pRE107	a suicide vector (<i>oriR6K</i> , RP4 <i>mob</i> , <i>sacB</i> , Ap ^r)	(61)
pCrcAT	<i>pagP</i> _{O157} in pGEM-T vector	this study
pWG24	<i>waaG</i> _{O157} cloned into pBAD24 (Amp ^R)	this study
pGU184	<i>galU</i> _{O157} cloned into pACYC184 (Cm ^R) [<i>pGalU</i>]	this study
pAA101	<i>E. coli galETK</i> cloned in pBR313	(41)
pACPagP	<i>E. coli pagP</i> cloned in pACYC184	(33)
pACPagPSer77Ala	Derivative of pACPagP	this study
pACPagP Δ 5-14	Previously pACPagP Δ 30-39 (precursor numbering)	(33)
pWQ3	<i>K. pneumoniae rfb</i> _{kp01} cloned in pRK404	(48)
pBAD-B2	<i>E. coli msbB2</i> cloned in pBAD24 [<i>pMsbB2</i>]	(19)
pEP24	<i>pagP</i> _{O157} in pBAD24	this study

^a Abbreviated descriptions used in some figures are included in square brackets.

Table 2. Minimal inhibitory concentrations of antibiotics in *E. coli* lipid A acylation mutants.

Strains	MIC ($\mu\text{g/ml}$) ^a	
	Vancomycin	Novobiocin
Wild-type O157:H7 4304	>100	>100
<i>pagP::aacC1</i>	>100	100
$\Delta\text{msbB1}, \Delta\text{msbB2}$	50	50
$\Delta\text{msbB1}, \Delta\text{msbB2}, \text{pagP::aacC1}$	25	3.125
Wild-type K-12 MC1061	>100	>100
<i>pagP::amp</i>	>100	>100
<i>msbB::Tn5</i>	>100	>100
<i>msbB::Tn5, pagP::amp</i>	>100	100

^a Minimal inhibitory concentration (MIC) was determined by a microdilution procedure using Mueller-Hinton broth as described in Experimental Procedures. The results are mean values of at least two independent experiments.

Table 3. Serum resistance associated with O157 polysaccharide.

Strains	Percentage of viable <i>E. coli</i> ^a		
	Time-zero	Time-1hour	Time-1hour (heat-inactivated)
Wild-type O157:H7 4304	100	96.6	97
$\Delta\text{msbB1}, \Delta\text{msbB2}$	100	30	88.3
$\Delta\text{msbB1}, \Delta\text{msbB2}, \text{pagP::aacC1}$	100	90.6	98.3
Wild-type K-12 MC1061	100	27.4	76

^a The numbers of *E. coli* were calculated as mean values of at least two independent experiments with the same non-immune calf serum as described in Experimental Procedures and percentages were determined in relation to the time-zero viable counts.

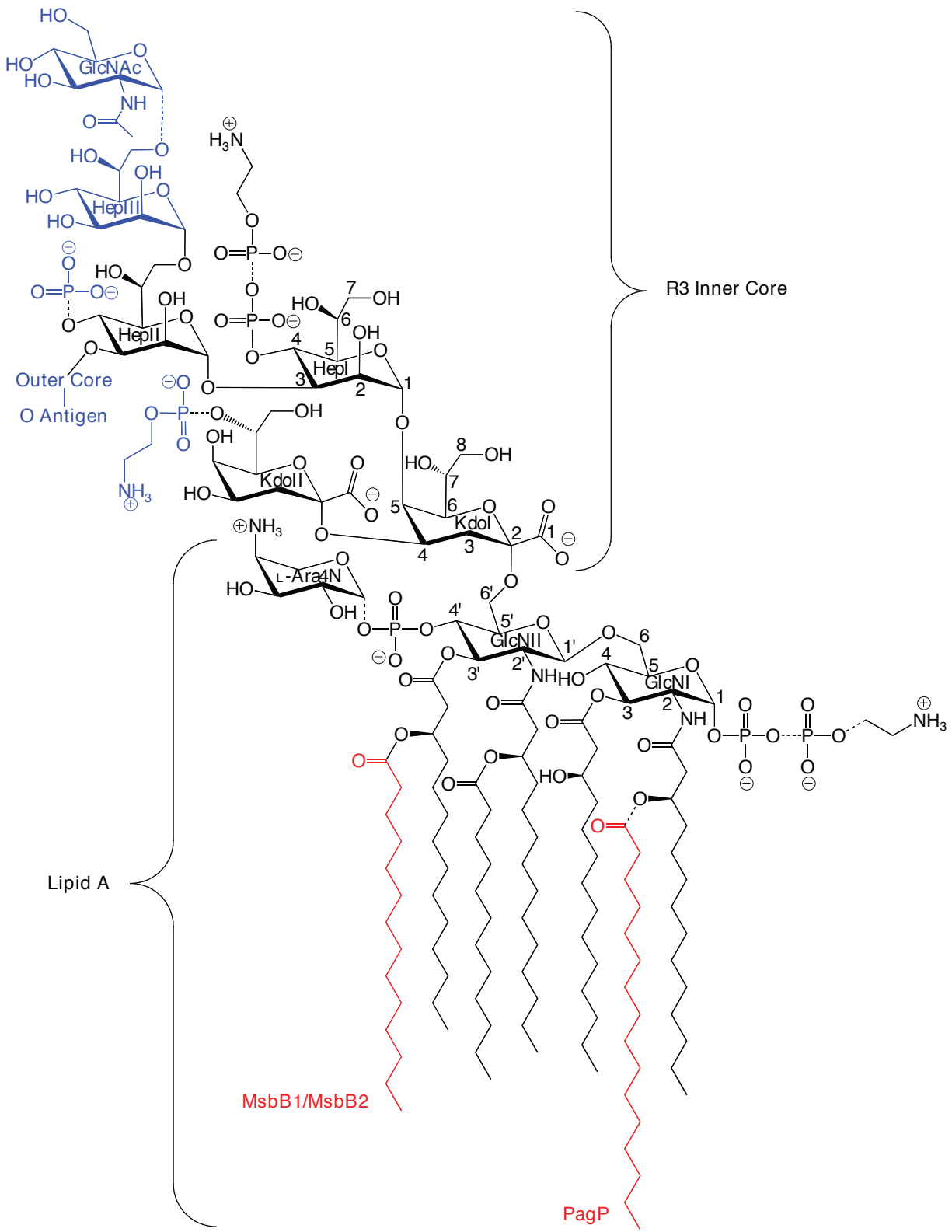
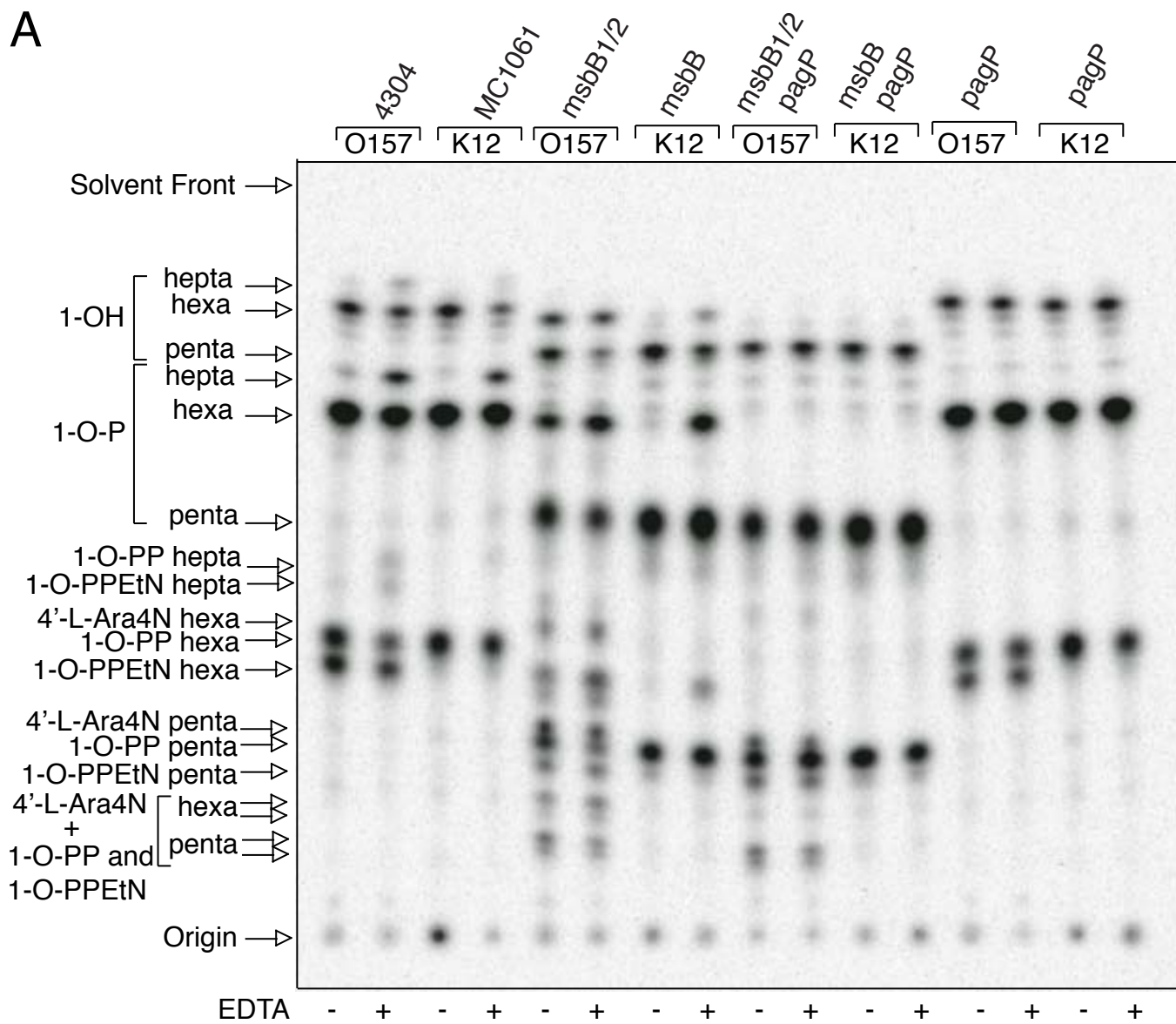


Figure 1

A



B

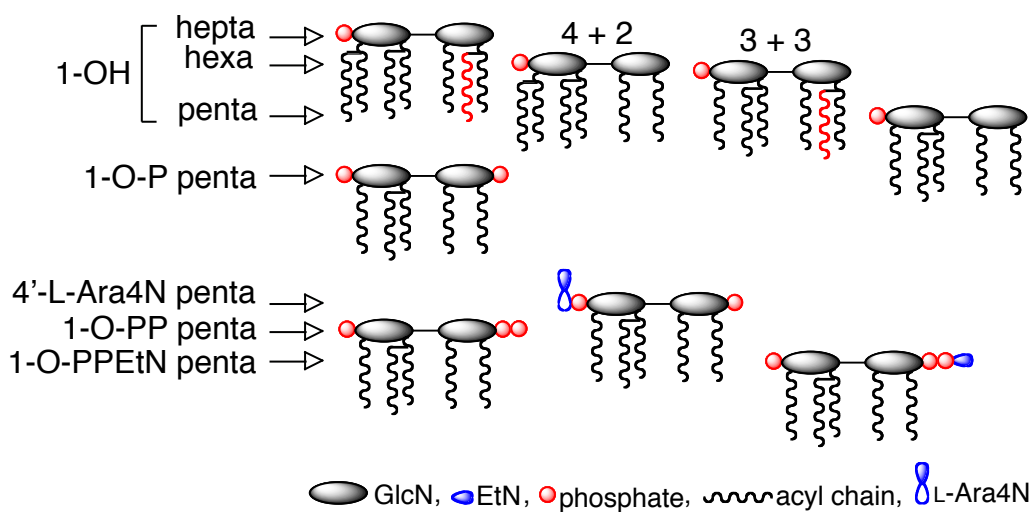


Figure 2

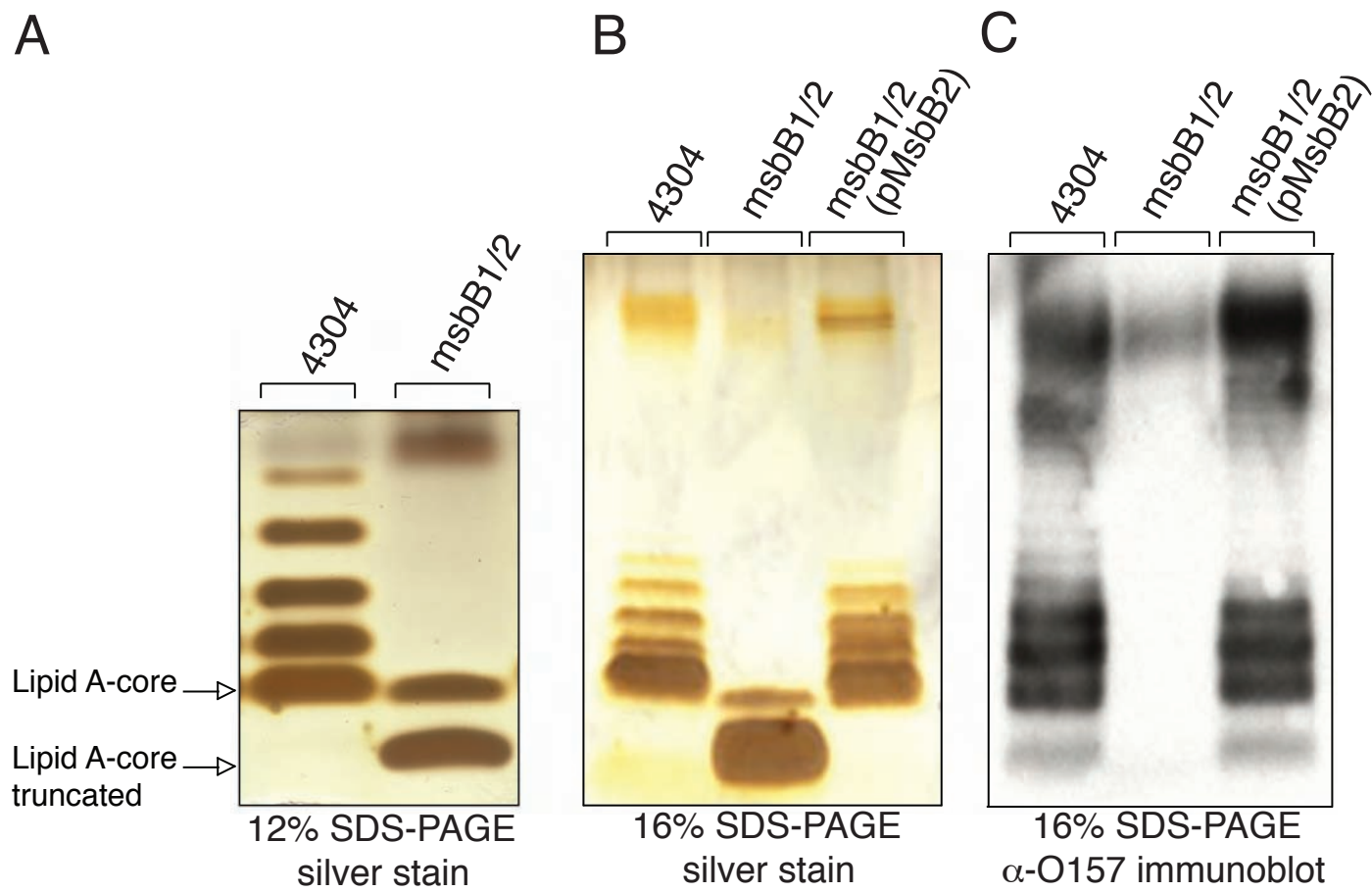
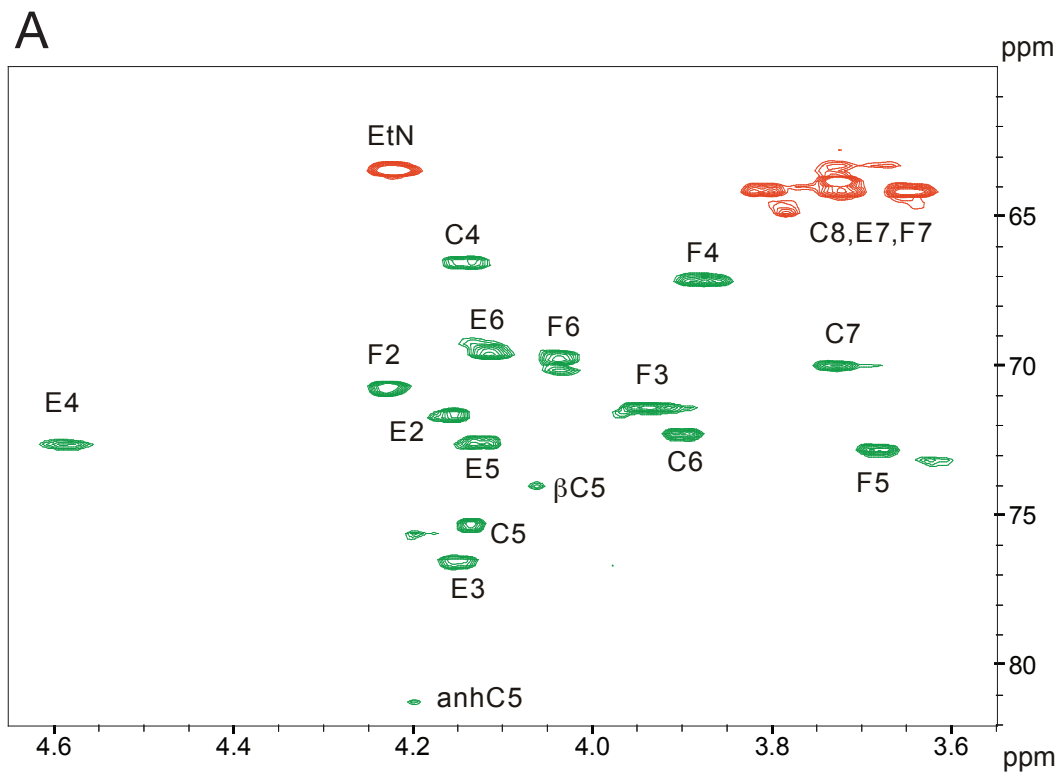


Figure 3

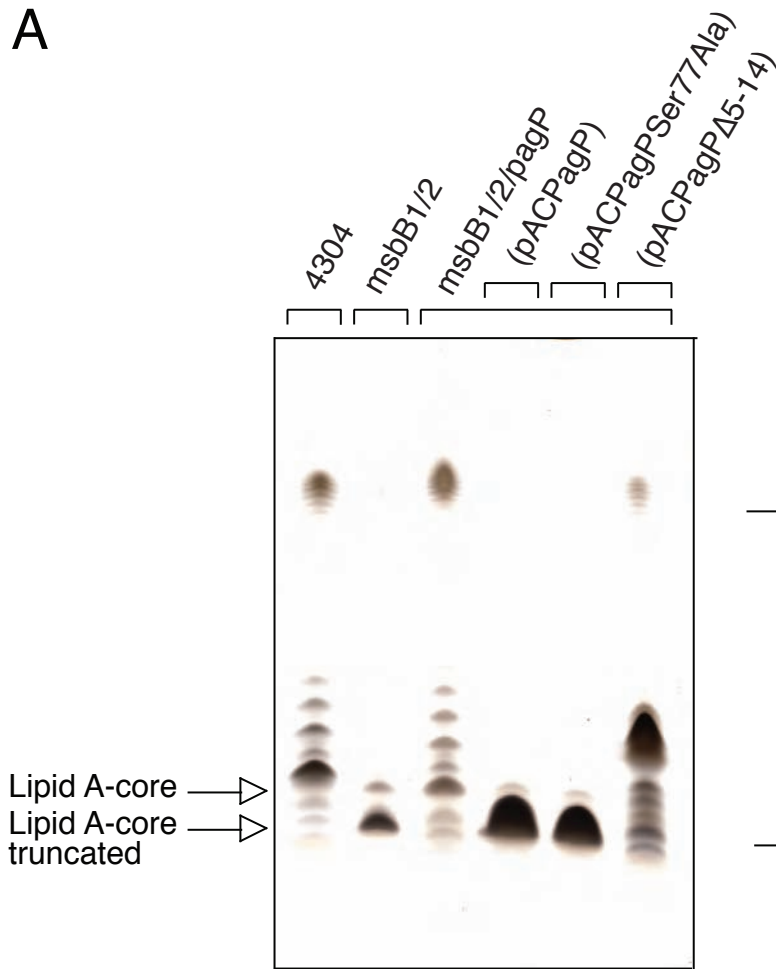


B

Unit	H/C 1	H/C 2/3a	H/C 3/3e	H/C 4	H/C 5	H/C 6	H/C 7	H/C 7'/8	H 8'
C		2.12	1.97	4.14	4.13	3.90	3.73	3.71	3.81
			34.8	66.4	75.2	72.2	69.9	64.0	
E	5.10	4.15	4.15	4.58	4.12	4.11	3.72	3.72	
	101.7	71.5	76.5	72.6	72.5	69.4	63.8		
F	5.19	4.23	3.94	3.88	3.68	4.04	3.64	3.72	
	102.9	70.7	71.3	67.1	72.7	69.6	64.1		
EtN	4.22	3.30							
	63.4	41.0							

Figure 4

A



B

Lipid A palmitate	-	+	-	+	-	+
Lipid A myristate	+	-	-	-	-	-
PagP helix	+	+	-	+	+	-

C

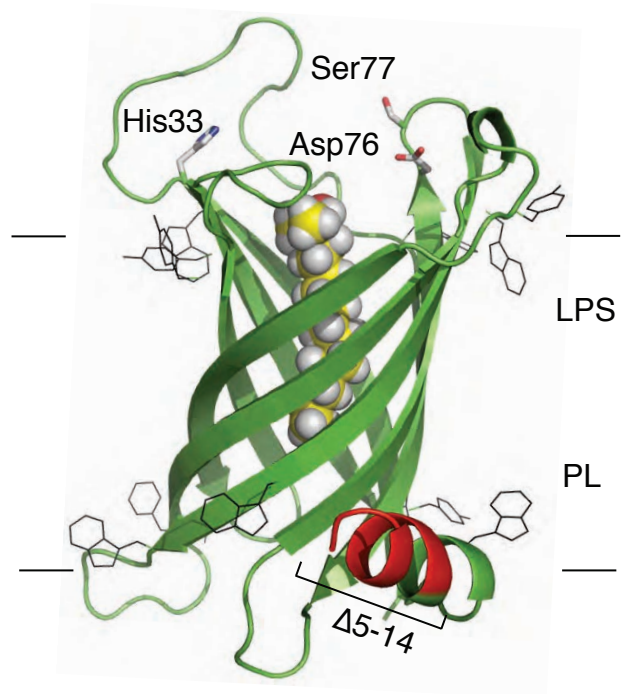


Figure 5

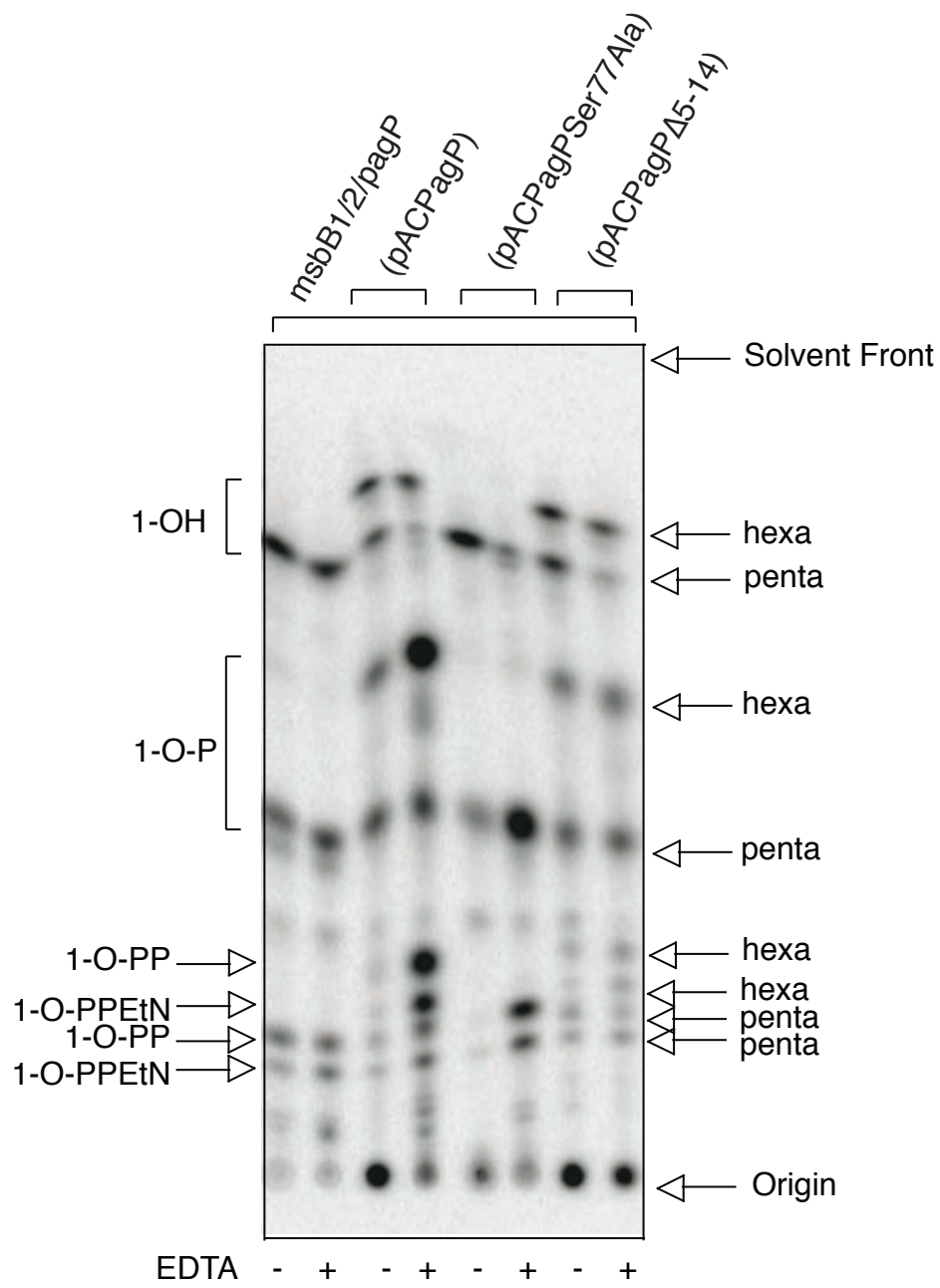


Figure 6

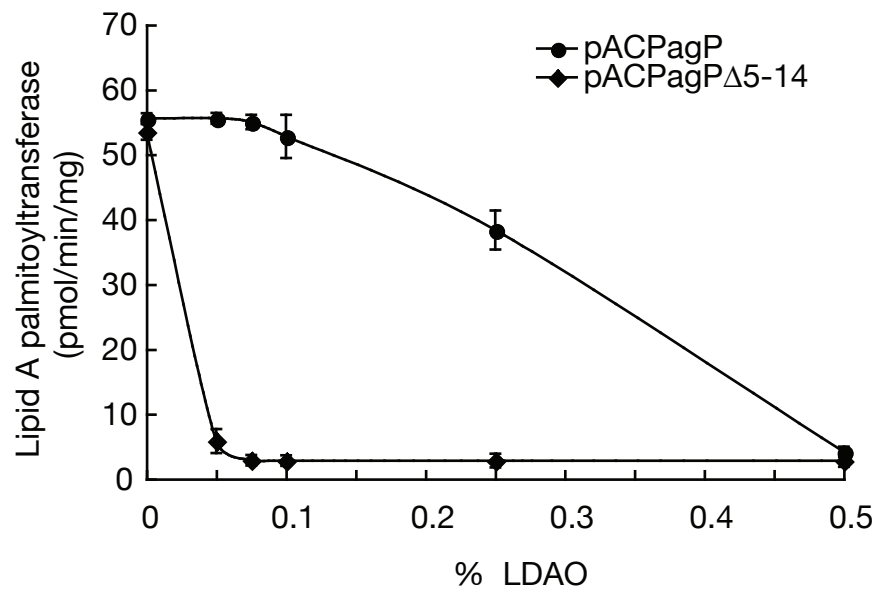


Figure 7

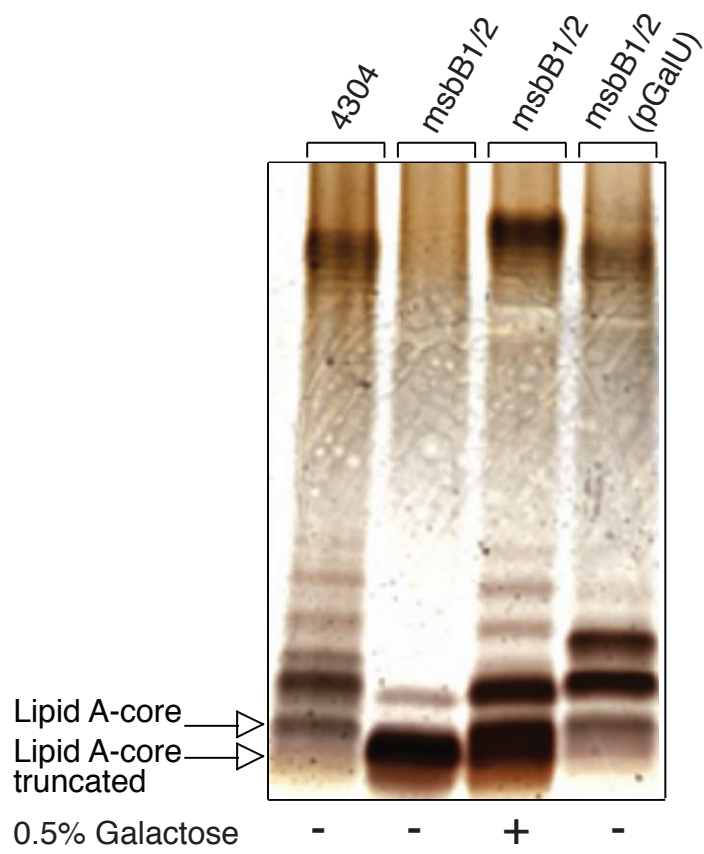


Figure 8

